

Local Transition to Turbulence in Electrohydrodynamic Convection

Shoichi Kai, Walter Zimmermann,^(a) Masanori Andoh, and Nobuyuki Chizumi

Department of Electrical Engineering, Kyushu Institute of Technology, Kitakyushu, Tobata 804, Japan

(Received 18 August 1989)

On the route to turbulence in electrohydrodynamic convection of nematic liquid crystals, the last bifurcation is spatially inhomogeneous via nucleation. Such a transition occurs between two different turbulent states (DSM1 and DSM2). We find good agreement between the nucleation rate of DSM2 nuclei and an expression from conventional nucleation theory. The motion of the DSM1-DSM2 interface behaves similarly to propagating fronts in other nonequilibrium systems. Disclinations in the director field are created during the transition, similar to the vortex filaments in the TI-TII transition in superfluid He II.

PACS numbers: 47.25.Ae, 47.20.Ky, 61.30.-v, 67.40.Hf

Turbulence occurs when sufficiently strong external fields are applied to a fluid system. For more than a century this has attracted great interest, and yet in many respects remains unsolved and is still a good candidate for surprise.¹ In small- as well as in large-aspect-ratio convection systems different routes to turbulence have been found.² However, for simple fluids in Rayleigh-Bénard convection or in Taylor-vortex flow on the route to turbulence the investigations are usually not done from a viewpoint of spatially local transitions, such as spontaneous nucleation phenomena.² A kind of local transition is known from plane Poiseuille flow³ and recently from the turbulence-turbulence transition in helium gas,⁴ but in both cases this is mainly induced by the boundaries.

When an external voltage is applied to a thin layer of nematic liquid crystals, electrohydrodynamic convection occurs above a first threshold voltage V_c .⁵ Immediately above V_c one mainly observes a well-ordered roll convection. However, at higher voltages one also observes, after a sequence of bifurcations, a transition to turbulence, which is traditionally called the dynamic scattering mode (DSM).⁵⁻⁷ Two different kinds of DSM have been observed, the DSM1 and DSM2 states,⁸⁻¹³ the DSM2 state occurs at a higher voltage above the threshold voltage, V_2 . Both states are characterized more quantitatively by measuring the spatial power spectra of the transmitted light, parallel (P_{\parallel}) and perpendicular (P_{\perp}) to the original director orientation.¹⁴ The wave-number dependences of P_{\parallel} and P_{\perp} are different from each other in DSM1 and become similar in DSM2. Therefore the notion of anisotropic (DSM1) and isotropic (DSM2) turbulence is used.¹⁴

Here we show that the transition between the two DSM states takes place via nucleation of small areas of DSM2 and their subsequent growth; the nucleation kinetics resembles nucleation in other nonconvective systems. During the growth of the DSM2 areas the motion of the DSM1-DSM2 interface is similar to propagating fronts in other nonequilibrium systems; however, we find an uncommon dependence of the interface velocity on the external control parameter. It is qualitatively dem-

onstrated that the disclination density in the director field characterizes the DSM1-DSM2 transition.

We have used the liquid-crystal material N-(*p*-methoxybenzylidene)-*p*-butylaniline (MBBA),¹⁴ which shows the nematic phase at both temperatures used in the experiment: 27 and 32 ± 0.1 °C. The experimental setup is the standard one;¹⁴ the electrodes extend here over 3.0×3.0 cm² and the thickness is $d = 50$ μm. We have measured with an applied voltage of 20 Hz, whereas the cutoff frequency was 170 Hz. In the present sample the onset for a roll convection (the Williams domains) is at $V_c = 6.8$ V and 27 °C.

In Fig. 1 the voltage dependence of the light transmittance ($=I/I_0$) through the sample is shown as a function of an increasing and a decreasing applied voltage with various ramp rates r (mV/s) in the neighborhood of the DSM1-DSM2 transition. I and I_0 are the light intensities passing through the sample in the presence of and in the absence of convection, respectively. The light transmittance (LT) in Fig. 1 has a sudden change in the slope at the voltage V_J . Above V_J the DSM2 nuclei are formed spontaneously. V_J is like an r -dependent DSM threshold. The voltage V_K in Fig. 1 is, however, rather insensitive to changes of r and the difference between V_J and V_K tends to zero for decreasing r . As shown in Fig. 2 the hysteresis gaps ΔV and $\Delta V^* = V_J - V_K$ exhibit a square-root dependence on r ; the solid (dotted) curve in Fig. 2 is calculated with ΔV (ΔV^*) $= (t_h r)^{1/2}$ by using the constant $t_h = 1.78 \times 10^3$ Vs ($t_h = 1.09 \times 10^3$ Vs). Because of this behavior we take V_K as the DSM2 threshold V_2 ($=31$ V at 27 °C) and the vanishing hysteresis in the LT indicates that the DSM1-DSM2 transition is supercritical.

An impression of the local behavior of the DSM1-DSM2 transition is given in Fig. 3. The photograph in Fig. 3(a) is taken immediately after a voltage jump from 0 to $\epsilon_2 = (V^2 - V_2^2)/V_2^2 = 8.0$; the dark regions are the spontaneously created DSM2 nuclei. With increasing time these nuclei grow [Fig. 3(b)] until there is fusion with other nuclei, and simultaneously new nuclei are created in the remaining DSM1 area until the whole area is in the DSM2 state [Fig. 3(c)]. The DSM2 nuclei

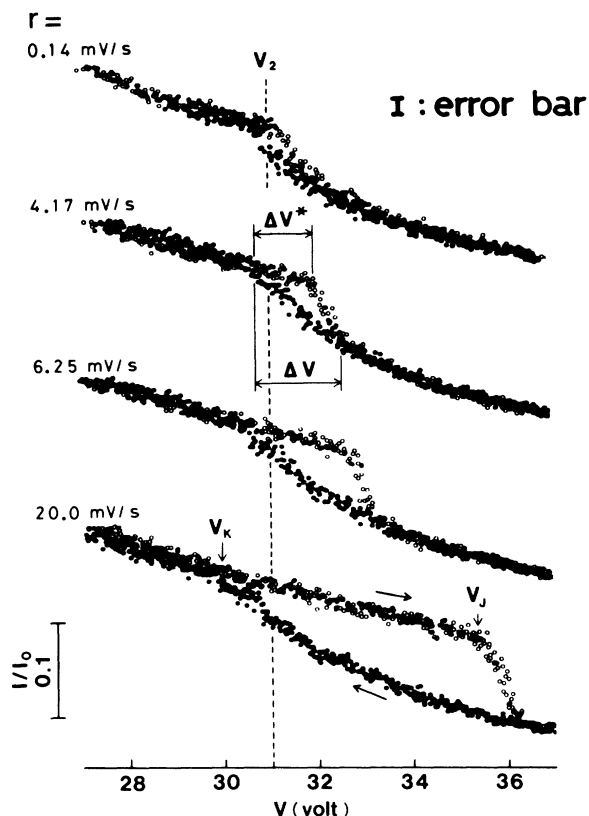


FIG. 1. Hysteresis in the light transmittance I/I_0 near the DSM1-DSM2 transition for various ramp rates r (mV/s) at $T=27^\circ\text{C}$. We choose two different hysteresis gaps ΔV and ΔV^* ($=V_J - V_K$). The open circles are obtained for increasing and the closed circles for decreasing voltage.

are always roughly elliptical, with the long axis parallel to the original undistorted director orientation. The number of nucleation sites increases and their size becomes smaller for larger ϵ_2 .

The number of DSM2 nuclei, which are spontaneously created at 1 to 2 s after the jump in the applied voltage from $V=0$ to a voltage above V_2 , is shown as a function of ϵ_2 in Fig. 4. From a conventional expression for the nucleation rates,¹⁵

$$J = J_\infty \exp[-A/(1 + \epsilon_2)] + B, \quad (1)$$

we obtain the curves in Fig. 4. The values $J_\infty = 920 \text{ mm}^{-2}$, $A = 50$, and $B = 1.4 \text{ mm}^{-2}$ for 27°C and 800, 25, and 0.9 for 32°C , respectively, are obtained for the best fit of Eq. (1) to the data in Fig. 4. Here A corresponds to the normalized activation energy and ϵ_2 is a measure of overstability in classical nucleation theory. B is probably related to heterogeneous nucleation, induced, e.g., by inhomogeneities at the electrodes. Repeating the experiment several times with long enough time for relaxation in between, the nucleation sites always occur randomly in space.

The main difference between the DSM1 and the

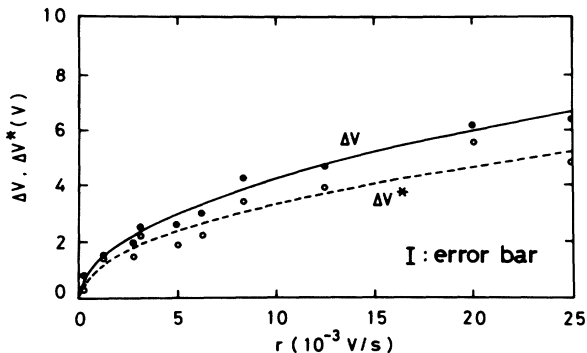


FIG. 2. The ramp-rate r dependence of the hysteresis gaps ΔV and ΔV^* as defined in Fig. 1. The solid curve is the expression $(t_h r)^{1/2}$ with $t_h = 1.78 \times 10^3 \text{ V s}$ and the dotted curve is for $t_h = 1.09 \times 10^3 \text{ V s}$.

DSM2 state is the density of disclinations in the director field, which is higher in DSM2. To visualize this, we use the fact that the relaxation of the flow field (velocity) and the simple director distortions is much faster than the relaxation of the disclinations in the DSM2 state. If we switch off the applied voltage $V > V_2$ at a time when the DSM2 state has already filled considerable space [Fig. 5(a)], then the disclinations can be clearly observed

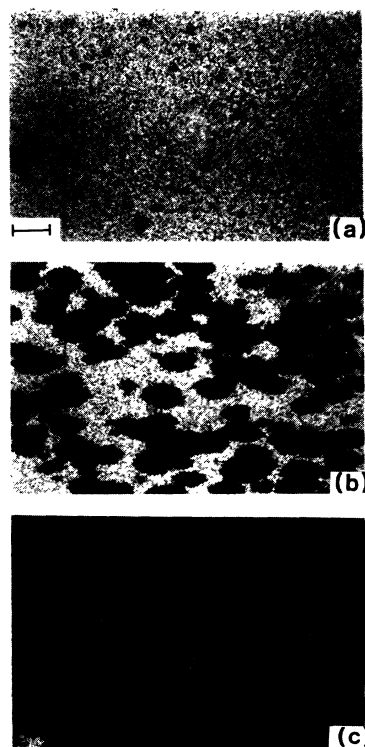


FIG. 3. A set of photographs of the growth process of DSM2 nuclei at different times after applying a voltage V larger than the DSM2 threshold voltage V_2 [$\epsilon_2 = (V^2 - V_2^2)/V_2^2 = 8.0$ and $T = 27^\circ\text{C}$]. (a) $t = 1 \text{ s}$, (b) 3 s , and (c) 6 s . The bar in (a) shows $500 \mu\text{m}$ in length.

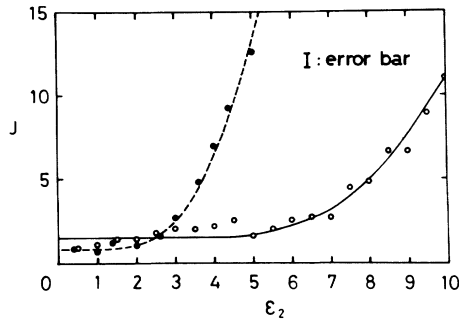


FIG. 4. Nucleation rate J for DSM2-turbulent nuclei as a function of ϵ_2 [$=(V^2 - V_2^2)/V_2^2$] for two different temperatures. \circ , 27°C; \bullet , 32°C. The solid and the dotted curves are due to Eq. (1).

in the areas where DSM2 was observed before, as shown in Fig. 5(b) and enlarged in Fig. 5(d). If we switch the voltage on again to above V_2 , before the disclinations have vanished, then the disclinations serve as nucleation centers for the DSM2 state and the same image as in Fig. 5(a) is obtained once more [Fig. 5(d)]. The disclination density in the DSM2 area itself increases with ϵ_2 (quantitative measurements of this density will be described elsewhere).

During the self-similar growth of the DSM2 nuclei, new disclinations are continuously created in the nuclei keeping the disclination density inside the nuclei roughly

constant. By measuring the diameters in the two main directions of the elliptical nuclei as a function of time, we always determine the growth velocities in a range where they become independent of the size of the nuclei. The ϵ_2 dependences of the velocities parallel (v_{\parallel}) and perpendicular (v_{\perp}) to the original director orientation are shown in Fig. 6 for the temperature $T=27^\circ\text{C}$. The curves show the expression $v = \gamma\epsilon^{0.7}$, where γ has been chosen for the best fit and has the values $\gamma=54 \mu\text{m/s}$ (v_{\parallel}), $29 \mu\text{m/s}$ (v_{\perp}) at 27°C and $65 \mu\text{m/s}$ (v_{\parallel}), $35 \mu\text{m/s}$ (v_{\perp}) at 32°C . The velocity ratio $v_{\parallel}/v_{\perp}=1.85$ is rather independent of ϵ_2 and is equal to the ratio of the diameters along the long and the short axes of the elliptical nuclei.

It is not possible to reverse the growth velocity of the nuclei by decreasing ϵ_2 below zero; instead the DSM2 state disperses away globally. In that respect the motion of the DSM1-DSM2 interface resembles propagating fronts in other nonequilibrium systems above a supercritical bifurcation (SB).¹⁶ The front velocity $v_s = \tau\epsilon_2^{0.5}/\xi$ above SB (where τ is a characteristic time and ξ is the coherence length), however, does not fit our experimental data. This is also the case for the front velocities from other deterministic equations related to the subcritical or the transcritical bifurcation discussed in Ref. 16 and simple extensions of those. At the DSM1-DSM2 bifurcation, mainly the disclination density is changed, indicating that it is the relevant order parameter. The flow field in both DSM regions is turbulent and the disclina-

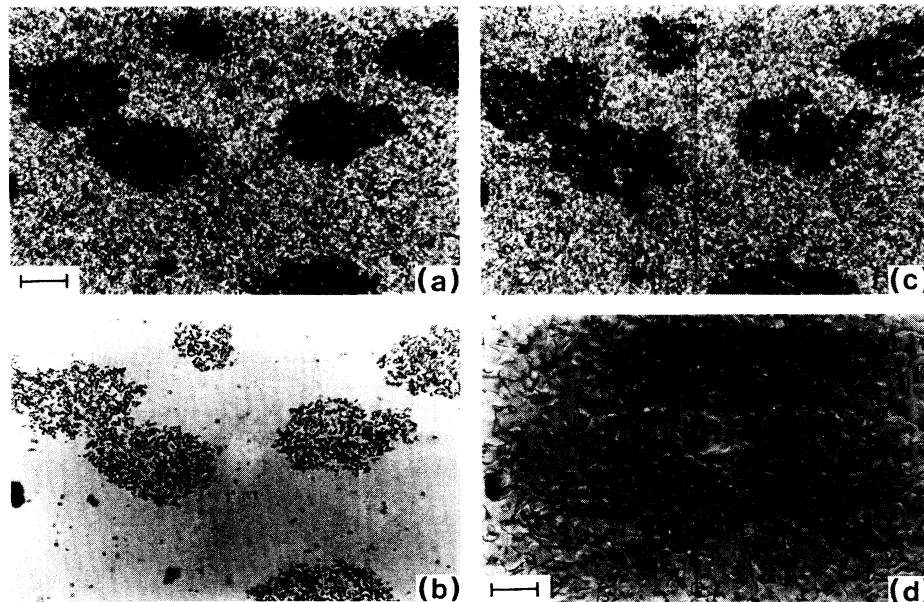


FIG. 5. Retriggering process of the DSM2 state by disclinations ($T=27^\circ\text{C}$). Photographs (a)–(c) are taken after a jump in the applied voltage above the thresholds, ϵ_2 [$=(V^2 - V_2^2)/V_2^2$]=1.04. (a) $t=24$ s after the jump, (b) $t=26$ s immediately after the field is switched off, (c) $t=28$ s immediately after the field is applied again, and (d) an enlargement of a disclination domain. The dark area shows the DSM2 state. In (b) a large number of disclinations can be seen in the domain where the DSM2 state existed before. (c) shows that the disclinations serve as DSM2 nucleation centers. The bars in (a) and (d) show 500 and 100 μm , respectively.

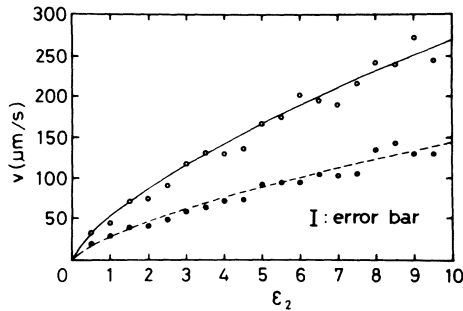


FIG. 6. The growth velocity of the DSM2 nuclei parallel $v_{||}$ (open circles) and perpendicular v_{\perp} (closed circles) to the original director orientation as function of ϵ_2 at 27°C. The curves are $\gamma\epsilon_2^{0.7}$, with $\gamma=54 \mu\text{m/s}$ ($v_{||}$) and $29 \mu\text{m/s}$ (v_{\perp}). For 32°C, similar results are obtained (Ref. 20).

tions are presumably formed by strong short-range fluctuations in the flow field via viscous coupling between the director and the flow field. It seems that the flow field acts like a destabilizing noise on the disclination-free director field. A realistic model for the DSM1-DSM2 transition should therefore at least include noise with a short correlation length, in contrast to the available deterministic models; if there is not an *ab initio* approach, starting from the full equations for electrohydrodynamics will be necessary. Investigations in this direction are in progress.

In conclusion, we have reported a local transition between two turbulent states DSM1 and DSM2 in electrohydrodynamic convection, which is rather uncommon for convective systems at supercritical bifurcations. The change in the disclination density, the divergence in the relaxation time,^{11,12} and the drastic increase of fluctuations of light intensity¹⁴ at the DSM1-DSM2 transition are similar to the properties of the TI-TII transition in superfluid He II, where the vortex filament density is changed during the bifurcation and where the transition is considered to be spatially homogeneous.¹⁷ We hope that the presented results stimulate further investigations, which can be complementary to, as well as an extension of the studies in He II. The influence of multiplicative noise on the DSM1-DSM2 transition seems especially promising,^{18,19} because it can also be applied in our system in a well controlled manner.¹⁸

(a)Present address: Institut für Festkörperforschung, Theorie III, Forschungszentrum Juelich Kernforschungsanlage, Postfach 1913, 5170 Juelich, Federal Republic of Germany.

¹For example, A. C. Monin and A. M. Yagom, *Statistical Hydrodynamics* (MIT Press, Boston, 1970), Vol. 1.

²H. L. Swinney and J. P. Gollub, *Hydrodynamic Instabilities and the Transition to Turbulence* (Springer-Verlag, Berlin, 1986), 2nd ed.

³M. Gad-El-Hak, R. F. Blackwelder, and J. J. Riley, *J. Fluid Mech.* **110**, 731 (1981); D. R. Carlson, S. E. Widnall, and M. F. Peeters, *J. Fluid Mech.* **121**, 487 (1982).

⁴F. Heslot, B. Casting, and A. Libchaber, *Phys. Rev. A* **36**, 5870 (1987).

⁵L. M. Blinov, *Electro-Optical and Magneto-Optical Properties of Liquid Crystals* (Wiley, New York, 1983); A. Joets and R. Ribotta, in *Cellular Structures in Instabilities*, edited by J. E. Wesfried and S. Zaleski (Springer-Verlag, Berlin, 1984).

⁶G. H. Heilmair, L. A. Zanoni, and L. Barton, *Proc. IEEE* **56**, 1162 (1968).

⁷S. Kai, in *Nonlinear Dynamical Systems*, edited by F. Moss and P. V. E. McClintock (Cambridge Univ. Press, Cambridge, 1989).

⁸A. Sussmann, *Appl. Phys. Lett.* **21**, 269 (1972).

⁹R. Chang, *J. Appl. Phys.* **44**, 1885 (1973).

¹⁰P. M. Alt and M. J. Freiser, *J. Appl. Phys.* **45**, 3237 (1974).

¹¹S. Kai and K. Hirakawa, *Solid State Commun.* **18**, 1573 (1976).

¹²S. Kai and K. Hirakawa, *Prog. Theor. Phys. Suppl.* **64**, 212 (1978).

¹³T. Krupkowski and W. Rusykievicz, *Mol. Cryst. Liq. Cryst.* **49**, 47 (1978).

¹⁴H. Yamazaki, S. Kai, and K. Hirakawa, *Mol. Cryst. Liq. Cryst.* **122**, 41 (1985).

¹⁵F. F. Abraham, *Homogeneous Nucleation Theory* (Academic, New York, 1974).

¹⁶E. Ben-Jacob, H. R. Brand, G. Dee, L. Kramer, and J. S. Langer, *Physica (Amsterdam)* **14D**, 348 (1985); W. van Saarloos, *Phys. Rev. A* **39**, 6367 (1989).

¹⁷J. T. Tough, in *Superfluid Turbulence in Low Temperature Physics*, edited by D. F. Brewer (North-Holland, Amsterdam, 1982), Vol. 8, p. 134.

¹⁸H. Brand, S. Kai, and S. Wakabayashi, *Phys. Rev. Lett.* **54**, 555 (1985).

¹⁹D. Griswold and J. T. Tough, *Phys. Rev. A* **36**, 1360 (1987).

²⁰S. Kai and W. Zimmermann, *Prog. Theor. Phys.* (to be published).

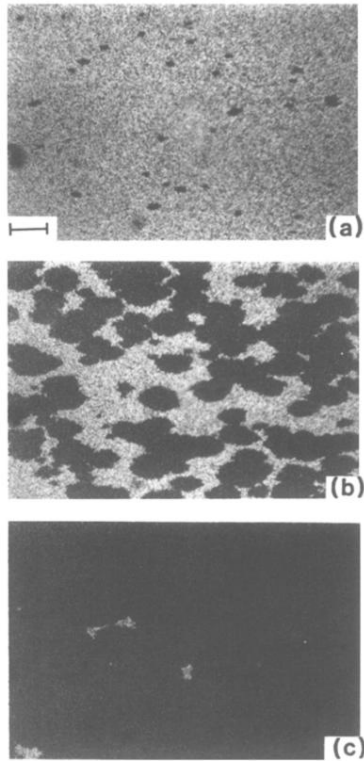


FIG. 3. A set of photographs of the growth process of DSM2 nuclei at different times after applying a voltage V larger than the DSM2 threshold voltage V_2 [$\epsilon_2 = (V^2 - V_2^2) / V_2^2 = 8.0$ and $T = 27^\circ\text{C}$]. (a) $t = 1$ s, (b) 3 s, and (c) 6 s. The bar in (a) shows $500\ \mu\text{m}$ in length.

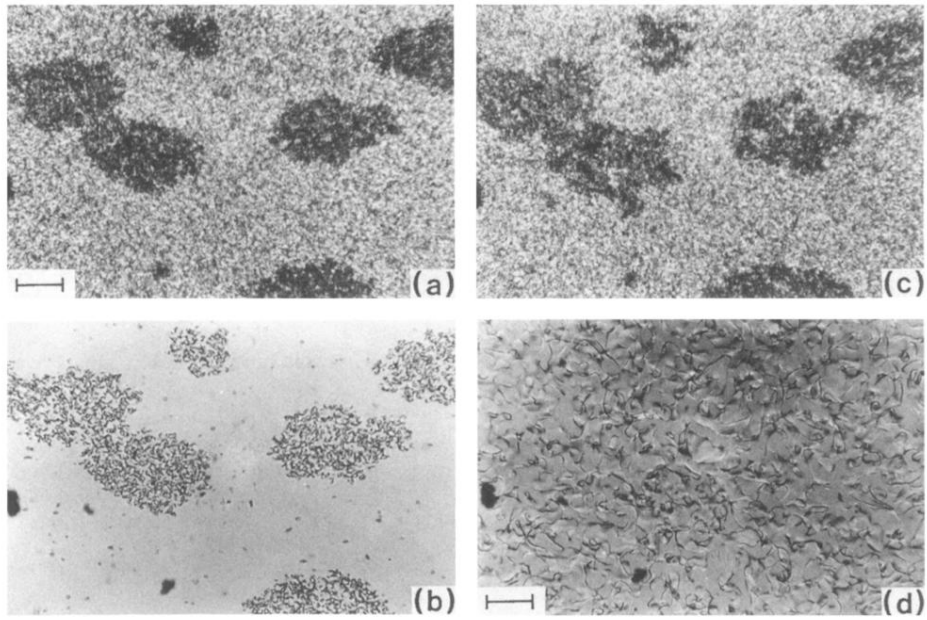


FIG. 5. Retriggering process of the DSM2 state by disclinations ($T=27^{\circ}\text{C}$). Photographs (a)–(c) are taken after a jump in the applied voltage above the thresholds, $\epsilon_2 [=(V^2 - V_2^2)/V_2^2]=1.04$. (a) $t=24$ s after the jump, (b) $t=26$ s immediately after the field is switched off, (c) $t=28$ s immediately after the field is applied again, and (d) an enlargement of a disclination domain. The dark area shows the DSM2 state. In (b) a large number of disclinations can be seen in the domain where the DSM2 state existed before. (c) shows that the disclinations serve as DSM2 nucleation centers. The bars in (a) and (d) show 500 and 100 μm , respectively.